

Joining Sound Event Detection and Localization Through Spatial Segregation

Ivo Trowitzsch, Christopher Schymura, Dorothea Kolossa, and Klaus Obermayer

Abstract—Identification and localization of sounds are both integral parts of computational auditory scene analysis. Although each can be solved separately, the goal of forming coherent auditory objects and achieving a comprehensive spatial scene understanding suggests pursuing a joint solution of the two problems. This work presents an approach that robustly binds localization with the detection of sound events in a binaural robotic system. Both tasks are joined through the use of spatial stream segregation which produces probabilistic time-frequency masks for individual sources attributable to separate locations, enabling segregated sound event detection operating on these streams. We use simulations of a comprehensive suite of test scenes with multiple co-occurring sound sources, and propose performance measures for systematic investigation of the impact of scene complexity on this segregated detection of sound types. Analyzing the effect of head orientation, we show how a robot can facilitate high performance through optimal head rotation. Furthermore, we investigate the performance of segregated detection given possible localization error as well as error in the estimation of number of active sources. Our analysis demonstrates that the proposed approach is an effective method to obtain joint sound event location and type information under a wide range of conditions.

I. INTRODUCTION

REALISTIC aural environments consist of numerous co-occurring different sounds emitted from sources distributed in space. Computational auditory scene analysis thus involves the development of models that draw information from audio streams and assign semantic labels to auditory objects. For instance, a robotic system that is specialized to search and rescue missions should be able to detect the presence of a fire, an alarm that is going off, screaming victims, or a crying baby, and localize them. Two key issues therefore are (a) detecting sound events and their types within that stream, commonly called audio or sound event detection (*SED*), and (b) localizing the corresponding sources emitting the sounds, denoted sound source localization (*SSL*). This work investigates the combination of the two: joint sound event localization and detection (*SELD*).

For comprehensive understanding of acoustic (or any) scenes, it is not only necessary to know what is there and where there is something, but instead to know *what is where*. However, coherently attributing “type” and “location” to auditory objects in scenes with multiple simultaneously active

sources is notably more difficult than performing *SED* or *SSL* individually, which is why there are only few works on the topic so far ([1]–[9]).

There are four different fundamental approaches to joining sound event detection and source localization:

1) *Temporal correlation*: Associating type and location of sounds through temporal correlation. This however is not possible for multiple sounds starting at the same time; and difficult for moving sources. If sources move (temporarily) to the same location, tracking gets lost.

2) *Sound-type masked SSL*: Attending to streams related to individual sound events. This “focus” can be created through masking the input such that a particular sound known to be active is “passed through” to *SSL*, and other sounds or noise are suppressed. Such masking is feasible in time-frequency domain if sound events exhibit specific frequency signatures. The subsequent localization then produces locations associative to these events. However, not all sound event classes exhibit coherent (and narrow) frequency signatures – for instance “alarm” is more of a semantic class, and can range from electronic beeps to fire bells; or “piano” ranges from very low to high frequencies. Also, the approach is likely to fail for co-occurring sound events with similar frequency patterns.

A work following this approach is presented in [3]. While the system is advertised and analyzed with regard to improving *SSL*, not *SELD*, it effectively joins sound event type and sound source location information.

3) *Spatially masked SED*: Attending to streams related to individual source locations. This implies masking of the input such that only sound from a particular direction is passed through to *SED*, and sound from other directions is suppressed. Such masking is technically doable in time domain through beam-forming, or in time-frequency domain through spatial segregation, attributing individual time-frequency-bins to particular directions. Sound events detected on the spatial streams are then associated with a location. Efficient masking depends on spatial separation of sources and hence dissimilar spatial cues.

Following approach 3, there is one work using beam-forming [5], and one comprehensive work [6] in which spatial masks are applied to the time-frequency feature space, on which a Gaussian mixture model (*GMM*) detects speech. [4] mix elements of approach 3 (beam-forming) and 2 (using prior sound event detection information on the full stream).

4) *Joint SELD*: Building models that by construction detect localized sound events. Such models do not localize and detect separately or subsequently (as in approaches 2 and 3), but

The authors IT and KO are with the Neural Information Processing Group, Department of Electrical Engineering and Computer Science, Technische Universität Berlin. The authors CS and DK are with the Cognitive Signal Processing Group, Department of Electrical Engineering and Information Technology, Ruhr-Universität Bochum.

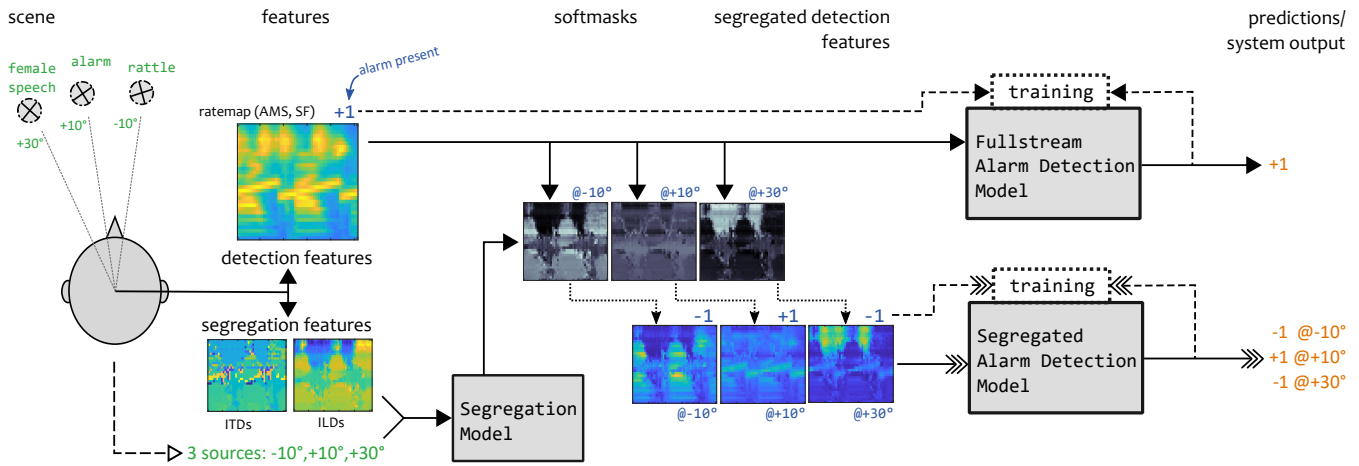


Fig. 1. From binaural scenes to localized detections. Exemplary scene with three sources, at -10° (emitting female speech), $+10^\circ$ (alarm sound), and $+30^\circ$ (rattling sound). From ear-signals, detection and segregation features are computed and cut into blocks of 500ms (amplitude modulation spectrograms (AMS) and spectral features (SF) omitted for clarity). Together with input about number of active sources and their azimuths (ground truth at training time, systematically perturbed or ground truth at testing time for our analysis; estimated or set values in a deployment system), the segregation model produces one softmask for each spatial stream, that is, for each azimuth. Each softmask gets applied to the detection features, such that one set of features is formed per stream. Labels about the presence of target sound events (alarm, in this case) are attached according to the associated azimuth. Segregated features are then input to the segregated detection models, which are trained to predict the presence of target events in the passed blocks (in the depicted example, all predictions are correct). Fullstream models, not part of the segregated detection but complementary and for comparison, get non-masked detection features and detect the presence of target events in the full mixture.

instead produce joint attributes from the start. While – because of the implicit combination of approaches 1-3 – this approach should in principle be the most powerful, it also requires the most powerful model, more difficult to train and to understand.

Three more recent publications present fully joint SELD systems following approach 4, all employing Deep Neural Networks (DNNs): [7] and [8] build speech detection and localization models, demonstrating the feasibility of training joint sound event detection and localization models based on DNNs [7] and Convolutional Neural Networks (CNNs) [8], although the former only with one source active at a time, and the latter with results difficult to judge, being restricted to overall averages. The so far most comprehensive paper on the topic [9] features a fully joint SELD system based on a Convolutional Recurrent Neural Network (CRNN) model.

In the present work, we are following approach 3, detecting sound events on spatially segregated streams. Apart from the immediately related works mentioned above, this approach is related to Blind Source Separation (BSS) techniques from the field of digital signal processing [10]–[14]. The employed spatial segregation model, computing softmasks in time-frequency space as similarly described in [3], [15], [16], serves as a processing step for associating auditory features later used for sound event detection with specific sound source locations.

Compared to approach 2, sound event detection on spatial streams has the advantage of enabling localized identification of multiple sources of the same type or with similar frequency ranges active. Compared to approach 4, this approach is feasible also with less powerful models classes, faster to train, and easier to understand. Furthermore, systems following approach 3 are modular, which enables work and research on the individual components.

We use the spatially masked auditory features for sound

event detection in a scheme called multi-conditional training, presented in [17] for robust binaural SED modeling. Although DNNs in various forms are predominant in sound event detection by now ([18]–[26]), we chose to stick to the lasso-models used in [17], which are very easy and fast to train and test. These models have shown to produce decent performance with the employed ratemap and amplitude modulation spectrogram features, and we opted to rather perform and provide extensive tests and qualitative analysis of the system instead of demonstrating the best performance possible.

Contrary to the related speech SELD system in [6], we decided to train the localized SED models with mask application *included* and multi-conditionally with overlapping sources, rather than training on clean data and applying masks during testing together with a missing data approach. Results of [6] show a strong dependence on signal-to-noise ratio (SNR) even in regimes with the noise exhibiting less energy than the target signal, and we believe that our data-driven approach potentially leads to more robust identification.

This work was started in the scope of the TWO!EARS Project (<http://twoears.eu>, [27]), which aimed for comparability to human performance and enabling a better computational understanding auditory and multi-modal perception. Hence, we restrict ourselves to *binaural* processing, simulating ear-signals of a humanoid robot. The only related articles covering binaural analysis are [3], [6]. Most commonly arrays with more than two microphones are used; in general spatial segregation and localization often rely on the availability of multiple microphones for maximum performance [8], [9], [28], [29].

We provide a comprehensive analysis of the resulting SELD system with regard to acoustic conditions — particularly the influence of spatial source distribution has not been studied

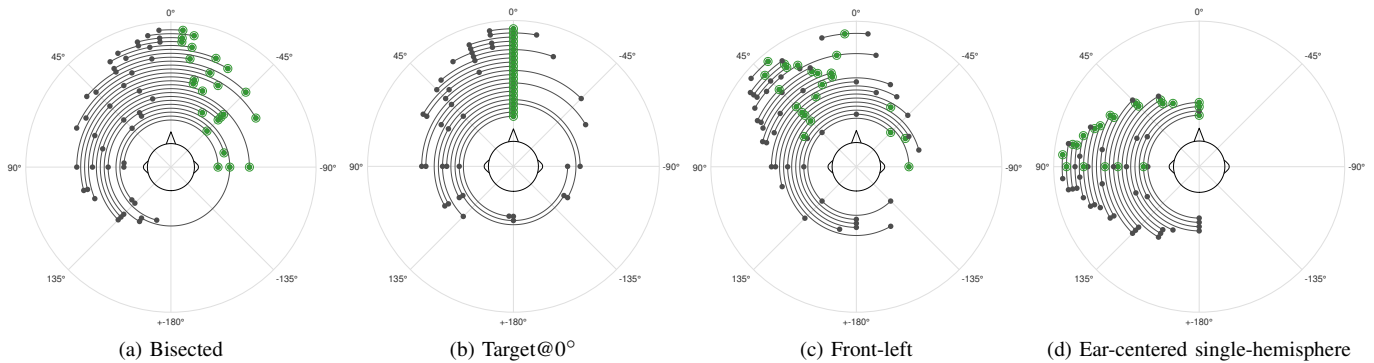


Fig. 2. Test scene configurations (only scenes with at least two sources), sorted into the different *scene modes*. Black filled circles depict distractor sources, target sources (green) are highlight by an enclosing open circle. Each scene is indicated by one circle fragment. The head is at the center.

before in this context — and dependency on correct input of number of active sources and quality of localization.

Our system as presented here is a proposition of how to join sound event detection and localization, and how to analyze and measure performance of such a system. The system and test scenes, together with the suggested performance measures, can serve as benchmarks for other SELD systems or components. Fig. 1 depicts the system and its information flow.

II. METHODS

A. Sound Data

The NIGENS database [30] was used to create the acoustic scenes for training and testing. This database provides audio files of 13 different event classes: alarm, crying baby, crash, barking dog, running engine, burning fire, footsteps, female speech, male speech, knocking, phone, piano, screams (we combined male and female screams into one class), and a “general” class with sounds of all kinds, exhibiting as much variety as possible. All sound events included are isolated without superposition of ambient or other foreground sources. The sound files are annotated with on- and offsets of the included sound events, many files include several event instances. The “general” sounds only served as negative examples for the classifiers and as distractor signals (see Sections II-B and II-F).

Containing 1017 wav files, NIGENS is the currently largest database of truly isolated sound events annotated with event on- and offset times.

B. Binaural Auditory Scenes

A set of binaural auditory scenes was rendered for training the detection models, and another set for testing. These scenes consist of different numbers of sound sources (one to four) at different locations — whenever the term location is used throughout this work, it refers to the azimuth relative to the head, disregarding distance and elevation.

To create the two-channel “ear signals”, we used the binaural simulator of the TWO!EARS system [31]. The simulator convolved the audio source with an anechoic head-related impulse response (HRIR) measured with a Knowles Electronic

Manikin for Acoustic Research (KEMAR) head, resulting in two-channel “ear signals” [32].

Binaural simulation was conducted for each source separately to allow control over the energy ratio of the sources *in the ear-signals*. To this end, the resulting ear-signal streams for each source were mixed at defined ratios of squared amplitudes averaged over both binaural channels and time, only including times of sound activity to not influence the ratio by periods of silence. We later refer to these ratios as SNRs even though there is no “classic” noise involved. The SNR was fixed such that it was the SNR of the “target” to each individual “distractor” source. Distractor sources never simultaneously emitted a sound from the same class as the sound emitted by the target source. This way we were able to control event-wise SNRs and evaluate systematically.

Eighty training scenes were defined for multi-conditional training, as introduced in [17]. However, due to the increased number of free parameters of scenes with more than two sources, it seemed more efficient to randomly sample the parameter space compared to manual definition of scenes. We randomly chose

- the number of sources (one to four)
- the azimuths between head and sources (uniformly between $\pm 180^\circ$, discretized to 22.5° -steps¹)
- the SNRs between target and other sources (uniformly between -20 and $+20$ dB).

For *testing*, *468 scenes* were defined such that it would be possible to look at only one scene parameter changing and keeping the others constant — the high number of scenes compared to the training set is due to this constraint. The following parameters were varied:

- the number of sources (one to four)
- the SNRs between target and distractor sources (-20 dB, -10 dB, 0 dB, $+10$ dB, $+20$ dB)
- the azimuth difference between sources (0° , 10° , 20° , 45° , 60° , 90° , 120° , 180°)
- the “scene mode” (depicted in Fig. 2):

- 1) *bisecting*: the nose (0° azimuth) points between target and distractor source(s)

¹This discretization serves computation efficiency; 22.5° is a compromise between smaller number of renderings and more dense spatial sampling.

- 2) *target@0*: the nose points towards the target source
 - 3) *front-left*: sources are mainly between 0° and 90° ; they are not bisected and targets are not at 0° , and they are not symmetric around the ear
 - 4) *ear-centered*: sources are distributed in the left hemisphere symmetrically around the ear (90°)
- the position of the target among the sources: either at one end, or (only for three-source scenes²) at the center.

No differentiation was made between left and right, since head and scenes are symmetric.

For all scenes, each of the NIGENS files was used once as target source sound. Sounds shorter than 30s were looped.

Exact definitions of training and test scenes can be found in the supplementaries, as well as the code to replicate them together with AMLTTP [33] and NIGENS [30].

C. Spatial Stream Segregation

The general information flow concerning the stream segregation stage and its embedding into the segregated detection system is depicted in Fig. 1. Blocks of interaural time-differences (ITDs) and interaural level-differences (ILDs) in time-frequency-representation, as well as the estimated number of active sources with corresponding locations serve as inputs to the segregation model. At the core of the Spatial Stream Segregation (SSS) stage, generalized linear models (GLMs) [34] are used as mapping functions from azimuthal source location to prototypical ITD τ_{kl} and ILD δ_{kl} cues at each time frame k and frequency channel l . These cues are combined into two-dimensional binaural observation vectors $\tilde{\mathbf{y}}_{kl} = [\tau_{kl} \ \delta_{kl}]^T$. The underlying observation models are represented as

$$\mathbf{y}_{kl} = \mathbf{g}_l(\phi) + \mathbf{n}_{kl}, \quad (1)$$

where $\mathbf{g}_l(\phi)$ is a mapping function of an azimuth angle ϕ and $\mathbf{n}_{kl} \sim \mathcal{N}(\mathbf{0}, \mathbf{R}_l)$ is an additive Gaussian noise term with frequency-dependent covariance matrix \mathbf{R}_l . The mapping function is realized as a GLM

$$\mathbf{g}_l(\phi) = \begin{bmatrix} \beta_{l0}^\tau + \sum_{n=1}^N \beta_{ln}^\tau \sin(n \cdot \phi) \\ \beta_{l0}^\delta + \sum_{n=1}^N \beta_{ln}^\delta \sin(n \cdot \phi) \end{bmatrix}, \quad (2)$$

which is based on trigonometric functions to account for the circular nature of the azimuthal source positions. Herein, N is the maximum order of the regression function and $\beta_{ln}^{\{\tau, \delta\}}$ represent the regression coefficients, which are estimated via linear regression using anechoic HRIRs [32] with white noise as stimulus signals. The residuals obtained after training are used to estimate the noise covariance matrix \mathbf{R}_l . The best-fitting model order N was determined using a selection process based on the Bayesian information criterion (BIC) [35].

Given a set of M estimated azimuthal source locations $\{\phi_i\}_{i=1}^M$ and corresponding binaural observations $\tilde{\mathbf{y}}_{kl}$, the model described in Eqs. (1) and (2) produces a softmask

weighting factor for the i -th source at time-step k and frequency-channel l according to

$$m_{kl}^{(i)} = \frac{p(\tilde{\mathbf{y}}_{kl} | \mathbf{g}(\phi_i), \mathbf{R}_l)}{\sum_{j=1}^M p(\tilde{\mathbf{y}}_{kl} | \mathbf{g}(\phi_j), \mathbf{R}_l)}. \quad (3)$$

An example of softmasks produced by Eq. (3) is depicted in Fig. 1.

D. Fullstream Detection Model Input

The simulated binaural auditory scenes were processed by the auditory front-end of the TWO!EARS system [31] to obtain the following representations:

- *ratemaps*: spectrograms resembling auditory nerve firing rates. Ratemaps are computed by smoothing the gammatone-filtered (32 channel) inner-hair-cell signal with a leaky integrator and binning into overlapping frames of 20 ms length (10 ms shift). [6], [36]–[38]
- *spectral features*: 14 different features summarizing the spectral content of the ratemap for each time frame: Centroid, Spread, Brightness, High-frequency content, Crest, Decrease, Entropy, Flatness, Irregularity, Kurtosis, Skewness, Roll-off, Flux, Variation. [39]–[45]
- *amplitude modulation spectrogram*: Each channel of the inner-hair-cell representation is analyzed by a bank of logarithmically scaled modulation filters. We used 16 *frequency channels* and 8 *modulation filters*. [46], [47]

For all representations, gammatone center frequencies ranged from 80 Hz to 8 kHz linearly spaced on the ERB scale.

All representations were split into overlapping blocks of 500ms (with a shift length of 333ms). For each block, a feature vector was constructed as input to the sound type classification: first, representations were averaged over left and right channels³, and the first two discrete time derivatives were computed. Features were then aggregated from L-statistics⁴ (L-mean, L-scale, L-skewness, L-kurtosis) computed over time. This amounted to 1,091 dimensions per feature vector⁵.

Sound event onset and offset times were used to label each block (and thus corresponding feature vector) according to whether the target class was present (+1) or absent (-1) within the block. A sound event was defined present if either it occupied at least 75% of a block, or (for short events), if at least 75% of the sound event was included in the block. Blocks with occupation of less than these 75%, but more than 0%, were excluded from training and testing because we considered them ambiguous.

E. Segregated Detection Model Input

Segregating into spatial streams takes place after the generation of the different auditory representations and their segmentation into blocks (see Section II-D), and before the construction of feature vectors from the blocked auditory representations.

³In [17], channel-average features are compared with two-channel features.

⁴L-statistics[48] are shown to be more robust than conventional statistics, particularly for higher moments and little data [49, Ch. 9].

⁵For details of the feature construction see supplementary informations.

²Only for three-source scenes to save computation time.

The segregation model produces a set of probabilistic time-frequency soft-masks, with the number of masks corresponding to the number of active sources in the scene⁶. A source was defined active in a block if its mean energy in that block was above -40 dB of its whole-scene maximum energy.

These masks were applied (through multiplication) to the ratemaps and amplitude modulation spectrograms; spectral features were then computed from the masked ratemaps. Hence, one set of masked representations per spatial stream was produced, such that one feature vector per spatial stream could be generated. Fig. 1 summarizes the data processing steps.

Since each mask is generated based on a presumed location of active sound source(s), each mask is associated with this particular location. Ergo, each feature vector for the detection model is attributable to this location — and hence each detection itself, which is why we also call the output of the segregated detection models also localized detection.

Both for training the detection models and testing their performance, labels indicating the presence or absence of target sound types are needed. If a block was labeled negative (see Section II-D) before segregation, all segregated blocks were labeled negative. If a block was labeled positive before segregation, the segregated feature vector associated to the location *closest* to the target source was labeled positive, and the others negative.

F. Model Training

Two types of models were trained: *fullstream* detection models, operating on the full (mixed) stream, features, and labels as described in Section II-D, and *segregated detection* models, operating on the segregated streams, features, and labels as described in Section II-E. Apart from this difference in input and a difference in sample⁷ weighting (elaborated on below), both model types were trained identically, as described in this section.

In [17], the impact of superimposed distracting sources was systematically investigated, and demonstrated how robust models are obtained by including a range of conditions in the training data, a procedure called *multi-conditional training*. We used multi-conditional training over all 80 scenes for all our models in this work, extending it to an even wider range of included conditions (see Section II-B).

For all sound types, binary classifiers were trained in an one-vs-all scheme. As classifying model, the “Least Absolute Shrinkage and Selection Operator” (Lasso) [50] (utilizing the “GLMNET” package [51], [52]) was used, a linear logistic regression model with an L_1 penalty for the regression coefficients. This penalty leads to sparse models by forcing many regression coefficients to zero, making Lasso a classification method with an embedded feature selection procedure. For adjusting the regularization parameter λ (determining the strength of the L_1 regularization term) value, six-fold stratified cross-validation on the training set was performed. The value

⁶Actually of the number of locations with active sources (active spatial streams) — two sources at the same location have to count as one.

⁷The combination of a feature vector and the respective label is a *sample*.

with the best cross-validation performance was chosen and used to train the model on the full training set.

200k samples were used to actually train each model (due to memory restrictions of GLMNET)⁸, subsampled from the complete training set. The subsampling process enforced using equally many samples from each sound file’s mixture, so that long sound files would not be overrepresented in the training set. Samples were weighted in training such that the total sample weight of all samples from scenes with 1, 2, 3 and 4 sources, respectively, was equal.

All scene generation, data processing, model training and model testing was done using the open-source *Auditory Machine Learning Training and Testing Pipeline* [33], which wraps all steps described in Sections II-B to II-I.

G. Model Testing

Data were split into a training set for model building and a test set for estimating the generalization performance of the classifiers. To ensure that a block from the training set and a block from the test set never contained parts of the same sound file, training-test and cross-validation splits were conducted at the level of sound files. The set of sound files for each class (including the general class) was split into training set (75%) and test set (25%). Only the sounds from the training set were used to generate the auditory scenes for building the classification models, and only the sounds from the test set were used to generate the scenes for evaluating the prediction performance. The chosen ratio of training and test set balances between necessary training data to generate good models, and desirable predictive power of the test data. For both, the number of original sound files per class is the more essential parameter compared to the number of produced scenes from them.

While training was conducted multi-conditionally, tests were performed on individual scenes in order to conclude on relations between scene parameters and performances.

Blocks in which not all sources were *active* (since sources emit sounds that also exhibit silences), got removed to better reflect the influence of the number of sources. All remaining samples from the test set were used without further subsampling, amounting to about 12 million samples tested with each fullstream model and about 30 million with each segregated detection model.

H. Segregation Model Input Perturbation

As described in Sections II-C and II-E, the segregation model needs input on the number of active spatial streams and on their azimuths. For training, ground truth knowledge was used. For testing, we implemented three different modes:

- 1) Using ground truth for both data.
- 2) Using ground truth for the number of active streams, but perturbing the location information of those streams. This perturbation is conducted by adding random azimuth values drawn from a normal distribution with

⁸As the Lasso model has few free parameters (number of features + 1), this amount was enough. Actually performance saturated around 120k samples.

sigma of 5° , 10° , 20° , 45° , and 1000° to each block's location. The latter basically corresponds to drawing locations uniformly. Note that we did *not* change the sources' locations in the scenes, but *only the information about them* given as input to the segregation model, and hence the azimuth associated with a block.

- 3) Using ground truth for the locations of active streams, but perturbing the data about the active source number. A uniformly drawn random number between -2 and +2 was added to the number of streams ground truth (thresholding downwards at 1). In case of a reduction, the respective number of locations handed to the segregation model was removed randomly. In case of an increase, locations drawn randomly from a uniform distribution between 0° and 360° were added to the segregation model input.

I. Performance Measurement and Evaluation

Training and testing performance was measured utilizing balanced accuracy (BAC). As argued in [17], BAC is preferable over F-score and error rate because of their dependence on the data distribution — it is closer to an interpretation of “informedness” of a classifier. The same line of argumentation can be found in [53] promoting Bookmaker Informedness (also known as Youden's J Statistic [54]), which is a scaled equivalent of BAC.

For segregated detection training, BAC had to be adjusted: with this method, there exist many negative samples of points in time without positive present (as with fullstream negative samples) — in the following subindexed npp —, but there also exist negative samples of points in time with a positive present in another stream, in the following subindexed pp . These, however, have a much lower proportion than the npp negatives and would, if not up-weighted, have minor influence on training. This, consequently, would result in worse localized detection performance, because of too low cost of not discriminating between target and distractor streams. Thus, we defined BAC_{sw} (sw for stream-wise) for segregated detection:

$$\begin{aligned} BAC_{sw} &:= 0.5 \cdot SENS + 0.5 \cdot SPEC_{sw}, \text{ with} & (4) \\ SPEC_{sw} &:= 0.5 \cdot SPEC_{pp} + 0.5 \cdot SPEC_{npp}, \\ SENS &:= TP/(TP + FN), \\ SPEC &:= TN/(TN + FP). \end{aligned}$$

While BAC_{sw} summarizes performance in one number so that the models can be optimized, it is difficult to gain insight into the actual behavior of the models through that number. Two different aspects of segregated detection performance are interesting: time-wise detection performance, and localized detection performance.

1) *Time-wise Detection Evaluation*: To evaluate how well the system recognizes sound events irrespective of location and to compare performance to fullstream sound event detection models, we use time-wise measures, namely BAC_{tw} , mean of detection rate DR_{tw} and specificity $SPEC_{tw}$. To obtain these, we *aggregate* the segregated detection models' predictions over streams for each point in time: a positive prediction in any

TABLE I
MEASURES & NOMENCLATURE OVERVIEW

Pure detection	
BAC_{sw}	Stream-wise balanced accuracy (used for training). Mean of $SENS_{sw}$ and $SPEC_{sw}$
$SENS_{sw}$	Stream-wise sensitivity. Positive detection rate
$SPEC_{sw}$	Mean of $SPEC_{pp}$ and $SPEC_{npp}$
$SPEC_{pp}$	Specificity (negative class accuracy) of blocks (streams) that do not contain a target event, but at times at which in another stream, the target event is active
$SPEC_{npp}$	Specificity of blocks that do not contain a target event, at times at which the target event is inactive in all streams
Localized detection (all conditioned on target events being active and detected)	
$BAPR$	Best-assignment-possible rate. Proportion of sound event detections in the best-available (azimuth-wise) stream, but in no other stream
NEP	Number of excess positive assignments — amount of streams with false positive event detections
$AzmErr$	Mean azimuth error. Averages the azimuth distance of all positive-assigned streams to the correct azimuth
$Placement\ likelihood$	Depicts the average proportions of event detections in streams depending on their distance to the event's correct azimuth

stream produces an aggregate positive prediction. Hence, an aggregate negative prediction is constituted only if all streams are predicted negative. It is obvious that this can lead to an increase of the number of true positives as well as of false positives (shown and discussed in Sections III-A and III-B2).

The subindex tw indicates time-wise aggregate segregated detection performance, fs indicates fullstream models' performance.

2) *Localized Detection Evaluation*: To evaluate how well the system assigns detected sound events to the localized streams, we establish four measures that provide understanding of the behavior when a sound event is present and detected:

- The *placement likelihood* measures the average proportion of streams getting assigned positives, depending on their distance from the sound event's correct azimuth. Ideally, the placement likelihood would be 1 at the correct azimuth, and 0 everywhere else⁹.
- The *best-assignment-possible rate* ($BAPR$) describes how often the system assigns a positive to the stream with associated location *closest* to the true azimuth, and *only* to this stream. For unimpaired source-count and location input (see Section II-H), the closest stream is always the one with correct azimuth; for perturbed situations, it may well be a stream with azimuth distance greater than 0° .

⁹Only if the correct azimuth is actually always among the segregated streams, that is, for unperturbed data.

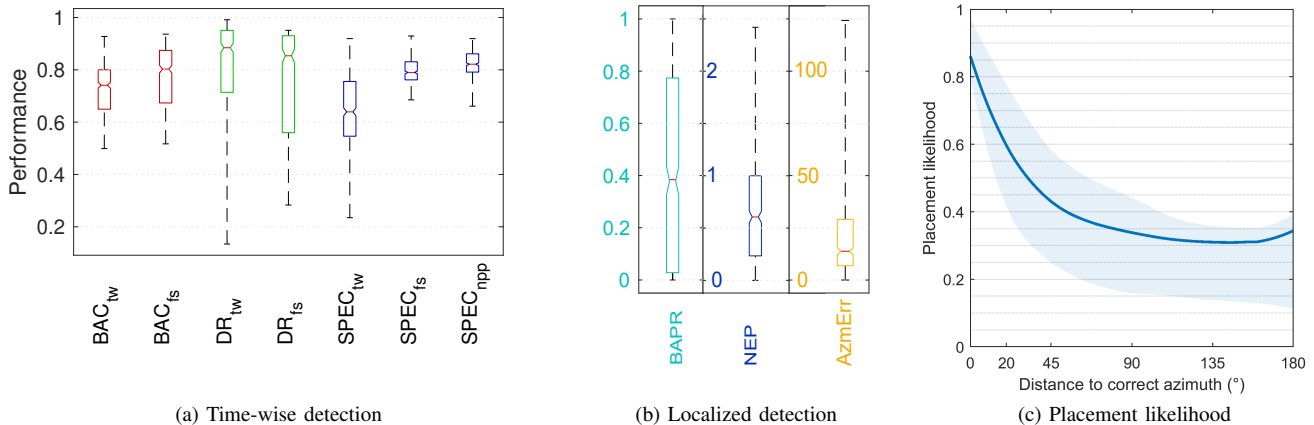


Fig. 3. Grand average (full test set, all test files, all classes) performances. Time-wise performances (a) are ignorant of location, providing detection performance *aggregated* over streams for segregated detection models, and comparing to fullstream models’ detection performance on the full mix. Localized detection performances (b,c) present measures regarding detection in the *correct* stream (that is, associated to the correct location). Boxplots indicate the 25th to 75th percentiles, the median and its 95% confidence interval, whiskers depict the complete range of values. The placement likelihood plot (c) displays the arithmetic mean and, shaded, the 25th to 75th percentiles. Table I or Section II-I provide descriptions of the presented measures.

TABLE II
GENERALIZATION: STREAM-WISE PERFORMANCES ON FULL TRAINING
AND TEST SET, AVERAGED OVER CLASSES AND ALL SCENES

Performance	test set mean	training set cross-validation mean
BAC_{sw}	0.777	0.806
$SENS_{sw}$	0.775	n.a.
$SPEC_{pp}$	0.649	n.a.
$SPEC_{npp}$	0.837	n.a.

- The *number of excess positive assignments (NEP)* indicates how many streams erroneously got assigned a positive. Ideally, this would be zero.
- The *mean azimuth error (AzmErr)* averages the distance of all positive-assigned streams to the correct azimuth.

Table I provides an overview over measures and nomenclature for easy later reference.

III. RESULTS AND EVALUATION

In Section III-A, we demonstrate the general functionality of the proposed method, followed by a discussion about the influence of the main acoustic scene parameters in Section III-B. In Sections III-C and III-D, the impact of estimation errors with respect to locations and number of sources is evaluated.

A. Method Functionality

Training produces functional models, as Table II shows. BAC_{sw} on the test set (averaged such that scenes with 1,2,3,4 sources have equal weight, as in training) is only a bit below training performance and well above chance level. ($SENS$, $SPEC_{pp}$ and $SPEC_{npp}$ constitute BAC_{sw} , cf. Section II-F.) Since different sounds and different scenes are used in the test set compared to the training set, this performance demonstrates successful generalization of the models.

Disassembling the surrogate performance number BAC_{sw} , in Fig. 3a, time-wise performances of segregated detection are

given and compared to fullstream detection. While being in the same range, the fullstream models do exhibit higher balanced accuracy. This is due to a notably worse specificity of the segregated detection models (median of 0.66, i.e. one out of three times, without a sound event present, the system actually assigns a positive to one or more streams) for which the better detection rate (median of 0.9, i.e. nine out of ten times, when a sound event is present, it is also detected) can not make up. This has to be carefully interpreted (see Section III-B2), since the additionally depicted underlying *stream-wise* $SPEC_{npp}$ of the segregated detection models is actually even a bit higher than the fullstream’s specificity.

The actual purpose of the segregated detection models is assigning sound events to the correct spatial stream. Figs. 3b and 3c show different indicators in this regard:

- Looking at the placement likelihood¹⁰, a sound event placement is most likely in a stream at the correct azimuth. This likelihood quickly drops with increasing azimuth distance up to around 60°. The ideal system would produce a peak at 0° only, but the graph shows that the method produces assignments more likely to be close to the true azimuth than far from it.
- The best-assignment-possible rate (BAPR) is, in the median, about 40%. That is, for the more difficult half of the scenes, between 0% and 40% of the event assignments are made to the correct stream (and only to it). For the easier half of the scenes, between 40% and 100% of the assignments are made to the correct stream (and only to it). The wide range indicates that scenes differ a lot in how well they can be segregated into localized streams; which is analyzed and discussed in Section III-B.
- The median azimuth error (AzmErr), giving the mean distance between the true sound event’s azimuth and the azimuths of its assigned streams, is about 13° and ranges

¹⁰This graph reads like: if there was a stream located at 20° distance to the true sound source’s azimuth, the mean proportion of blocks from this stream getting a positive sound event assignment would be 0.6.

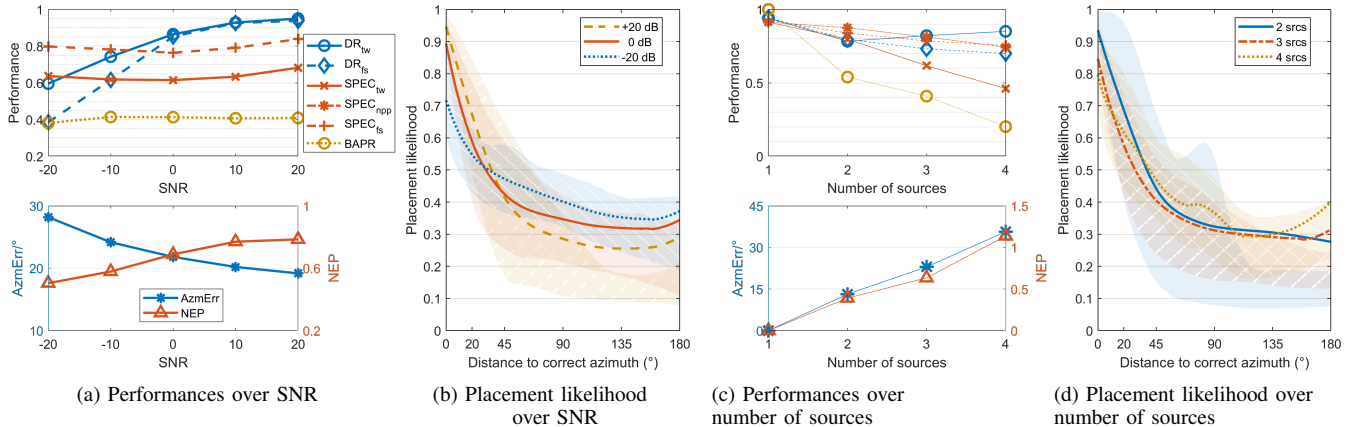


Fig. 4. Performances depending on SNR ((a),(b)) and number of sources ((c),(d)), averaged over all respective test scenes, all test files, and all classes. Line plots display arithmetic means and, shaded, 25th to 75th percentiles. Table I or Section II-I provide descriptions of the presented measures.

from 0° to 125° . This low average deviation is consistent with the placement likelihood plot, showing that most assignments are done close to the true azimuth.

- The median number of excess positive assignments (NEP) is 0.6. For about 25% of the scenes, only one stream is assigned a positive (which is ideal), but for the larger part of scenes, assignments to more than one stream occur frequently. Looking at the azimuth error, at least these excess assignments usually happen to streams close to the true azimuth.

B. Influence of Scene Configuration

The presented all-scenes grand average results exhibit a very wide range of performance. To investigate the factors influencing performance, three main scene configuration parameters are varied systematically across scenes in the following: the SNR between target and distractor sources, the number of distractor sources, and the scene mode.

1) *SNR*: The performance of the system over different SNRs is presented in Figs. 4a and 4b. For all SNRs, the same scene configurations are aggregated, hence the SNR is the only parameter varied.

Detection rate and specificity show typical behavior — DR_{tw} dropping with SNR, $SPEC_{tw}$ remaining mostly constant. Notable are the differences between segregated detection and fullstream models: the offset between specificities remains the same, while the detection rate differs only for difficult SNRs, where the segregated detection models perform better.

The number of positively assigned streams increases with SNR, because the stronger target source dominates the time-frequency space and more likely overrides ITDs and ILDs of the weak distractors. On the other side the mean azimuth error decreases with SNR, implying that — even though with more of them — the positive assignments at high SNRs are closer to the correct azimuth. The placement likelihood graph reflects this as well: up to about 30° azimuth distance, higher SNRs produce more (percentage-wise) assignments. Above about 30° , it reverses and higher SNRs of the target produce less assignments.

2) *Number of sources*: The performance of the system over different source counts is presented in Figs. 4c and 4d.

A clear negative correlation between number of sources and performance values can be observed, with the notable exception of the detection rate, which counter-intuitively increases slightly from two to four sources. For one and two sources, detection rate and specificity of segregated detection and fullstream models are very similar. The time-wise segregated detection $SPEC_{tw}$ however decreases for higher source counts much more strongly than $SPEC_{fs}$ — while the *block-wise* $SPEC_{npp}$ shows almost exactly the same behavior as $SPEC_{fs}$. This implies that the model's general ability to classify negatives is actually not lower than that of the fullstream models, and leads us to assume that the reason for both the strong decrease in time-wise specificity as well as for the increase in detection rate is actually the *successful segregation* into streams — which eases detection of positives, be they true, or be they false, due to sound similarity. In a *mix* of active sources, any positive (true or false) is less likely detected (this is shown by the detection rate of the fullstream model), but the segregation (to a certain extent) un-mixes. Since all sounds apart from the target class sounds are emitted from all distractor sources, higher number of sources mean higher probability of (false) positive occurrences. Hence, the time-wise aggregation over streams produces an increase in detection rate through true or false positives, and a decrease in specificity through false positives. This is an effect we deem practically unavoidable. In order to re-balance performance between time-wise detection rate and specificity to increase precision, it may be an option to adjust the training performance measure (BAC_{sw}) such that the weight of specificity is increased beyond 0.5.

The indicators of localized detection performance, $BAPR$, $AzmErr$ and NEP , all show lower performance for higher number of sources. This is to be expected, since more sources imply more overlap in time-frequency-space and thus less distinct segregation masks. In the placement likelihood graph, this is difficult to observe, because the means are very similar, but it can be noted by looking at the shaded indications of the

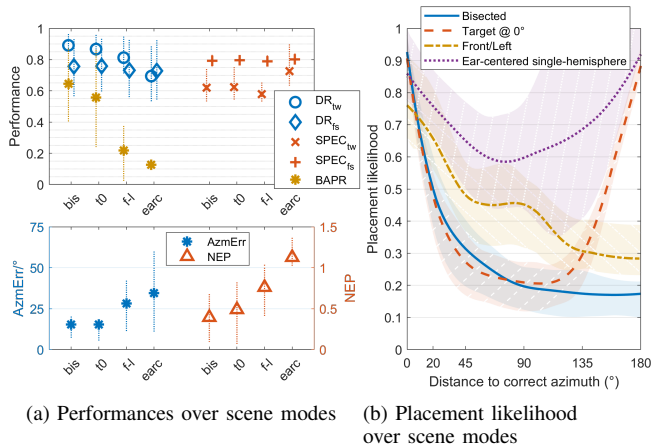


Fig. 5. Performances depending on scene mode, averaged over all respective test scenes, all test files, and all classes. Line plots display arithmetic means and, as dotted vertical lines, 25th to 75th percentiles. Table I or Section II-I provide descriptions of the presented measures.

25th to 75th percentiles.

3) *Scene mode*: The performance of the system for the four different scene modes (cf. Section II-B) are presented in Fig. 5. A clear gradation can be observed, with the bisected and target@0 modes performing best, front-left scenes performing worse and ear-centered-single-hemisphere scenes performing by far worst. This holds for all performance indicators apart from specificity. Although for the fullstream models the scene mode is far less influential (since the spatial features are not used there), on a much lower scale the same pattern can be noted for the detection rate.

For scenes in bisected or target@0 modes, *BAPR* is high and *AzmErr* is low (about 60% of all cases with the optimal assignment, and around 15° mean azimuth error), and few excess positives are assigned.

Particularly the latter increase strongly for the other two modes (negatively correlating *BAPR*) due to the increased occurrence of front-back-confusions. Front-back-confusions emerge because of the (approximate) front-back-symmetry of the head, which leads to similar spatial features for azimuths symmetric to the ear axis [55]. The employed segregation model for this reason actually disregards differences between front and back at all, in favor of more robust segregation in the frontal hemisphere (cf. Section II-C); any ear-symmetric scene hence must produce equal softmasks and result in the same classification of the symmetric streams.

The placement likelihood graph shows these effects very clearly. The bisected mode shows a curve close to the ideal, while the ear-centered curve demonstrates a severe lack of discrimination between locations for event assignments. Scenes with target at 0° show similar behavior as bisecting ones, but exhibit front-back-confusion approaching 180° .

While SNR and number of sources are unchangeable attributes of a given scene, the scene mode *is* changeable by head rotation. At least in a scene with sources changing positions slower than the head can turn, it should be possible to notably increase performance by choosing the look direction such that the sources of interest are spread as wide as possible

throughout the frontal hemisphere, optimally bisected. This is in accordance with results about dynamically improving localization performance in a binaural robot system [55].

C. Detector Performance and Localization Deviation

The segregation model relies on knowledge of two scene configuration attributes: the number of active sources and the locations (azimuths) of those sources. For the results above, both model inputs have been fed with ground truth. Since a real system likely would not (always) produce correct information about these two aspects, we conducted experiments with systematically perturbed values.

This section analyzes the influence of perturbation of the location input. The locations fed into the segregation model have an added random Gaussian component (see Section II-H) with different variances between 5° and 45° . Additionally, tests were performed with completely random azimuth input. For each individual variance, models were tested again on all test scenes and sound files and analyzed as before.

Fig. 6 shows the performances over localization error. Looking at the time-wise detection performance, it is notable that detection rate and specificity behave inversely, and both only change on a small scale (about ± 0.03).

The segregated detection performance indicators show stronger dependency on localization. The best-assignment-possible rate of the four different scene modes (cf. Sections II-B and III-B3) converge toward similar (low) values with increasing localization error — particularly the two well-performing modes (bisecting and target@0) decrease strongly. Interestingly, with random localization, the ear-centered scene mode exhibits the best *BAPR*, standing out from the other three modes¹¹. This can not lead to head turning rules of course, because with random localization, a robot would not know how to position sources at the ear.

Since the performance order of the four modes remains stable up to very high localization errors, the head turning guiding principle deduced in Section III-B3 stays valid, albeit with lower resulting performance gain.

The straight increase of *AzmErr* with localization error is logical — actually, the localization error does not even fully add to the system-inherent (at 0° localization error) azimuth error of about 22° .

D. Dependence on Number of Sources Estimation

After localization error, we analyze the impact of incorrect input of the number of active sources. To this end, we added an error of ± 2 to the source count and accordingly produced streams by the segregation model.

Fig. 7 shows performance over source count error — it is apparent that deviations from the correct number of streams bear strong performance changes. Time-wise detection rate and specificity show anti-correlated behavior: for underestimation of number of sources, the detection rate degrades heavily,

¹¹This is because for target sources at 90° , which occur in this scene mode, the probability of any spatial stream with random location getting a similar mask is least. (Highest for 0°)

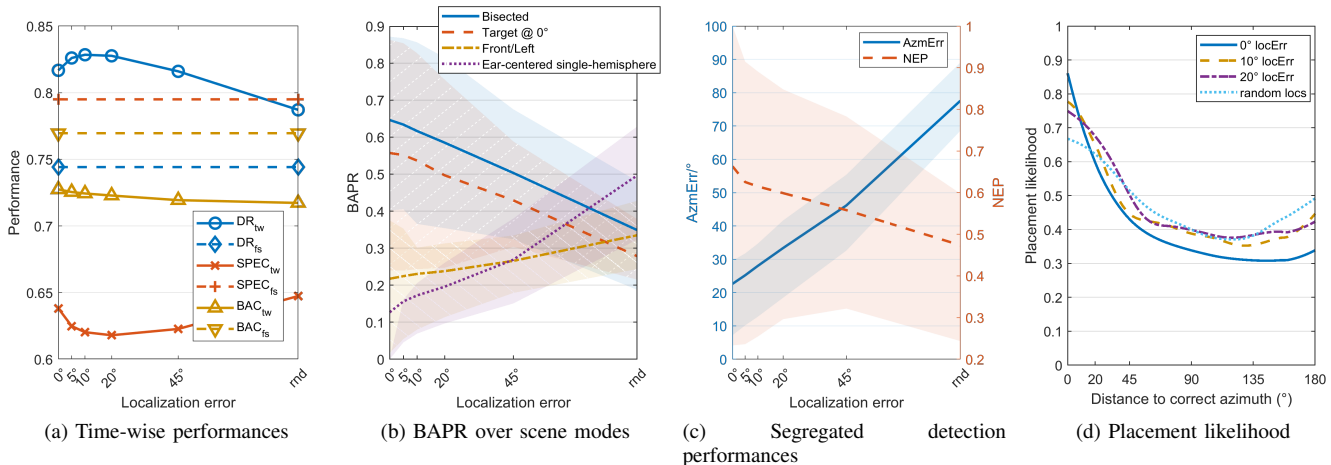


Fig. 6. Grand average (full test set, all test files, all classes) performances depending on strength of perturbation of location information fed into the segregation model. Localization error is given as standard deviation of the Gaussian perturbation added onto true azimuths, “rnd” standing for “random”. Line plots display arithmetic means and, shaded, 25th to 75th percentiles. Table I or Section II-I provide descriptions of the presented measures.

for overestimation of the source count, specificity drops even more.

Azimuth error and placement likelihood show that segregating into the wrong number of streams in both directions leads to worse localized detection performance. The azimuth error rises with any deviation: with too few streams, because the correct stream may be omitted, with too many streams, because segregation becomes more difficult and, as can be noted looking at *NEP*, because more excess positives are assigned.

The latter is also comprised in the strong decrease of *BAPR* for source count overestimation — any case of excess positive assignment is not a best-possible assignment. The increase of *BAPR* for negative source count error is no indicator of somehow better localized detection performance, but a mere logical consequence of the fact that with number of sources underestimation, scenes with two, respectively three, sources become segregated into one stream only, in which case the best-possible assignment is trivial.

Clearly the implication of these results is that the segregated detection system as proposed is dependent on an accurate estimation of number of active sources, but this is true of many systems in computational auditory scene analysis.

IV. DISCUSSION AND CONCLUSION

We have suggested and evaluated a method to annotate sound scenes with joint sound event type and location information in a binaural system. The proposed method combines spatial segregation in time-frequency-space with sound event detection on the segregated streams. Through this combination, the system helps forming coherent auditory objects with associated attributes location and type.

To achieve robustness with respect to varying scene conditions, we propose training multi-conditionally as in [17] and, importantly, to perform segregation already in training and not only in testing. The presented analysis demonstrates that this approach can produce localized sound type information

under a broad range of conditions and could be one core component of a binaural scene analysis system. The localized detection performance depends particularly on the number of active sources in the scene, and on their spatial distribution. By turning the head such that the sources of interest are in the frontal hemisphere (and at best bisected by the nose), the system’s performance in many situations can be increased strongly.

Proper estimation of the number of active spatial streams is a precondition of this approach; a deviation of more than one leads to very strong performance degradation. Localization error, on the other hand, does not influence segregated detection as heavily. Even with large errors, the system does not break down, but propagates the input error under mild impairment of assignment precision to the output.

The performance demonstrated was achieved by our system on short segments (500 ms), in contrast to the other works introduced following approach 3, which operate on the full events ([4]–[6]). Likely, using longer segments would increase performance on two ends: first, with longer blocks, sound events should become more identifiable (depending on the type). Second, longer blocks should make streams more segregable, because the strength of superposition varies strongly over time and hence longer blocks will include more frames with the individual sources standing out.

Certainly, the detection model class (logistic regression) is a limit to performance in our investigation. Pilot tests with nonlinear SVM (rbf kernels) and random forests did not improve performance — which led us to suppose that basic nonlinear information in the data is already extracted in the feature creation. However, it is reasonable to assume that more complex models able to model and integrate information over time, like CNNs or Recurrent Neural Networks (RNNs), would show higher performance. Nevertheless we expect results of our analysis to qualitatively carry over to more powerful model classes, since they depend mainly on the acoustic scene properties and the general construction of the method.

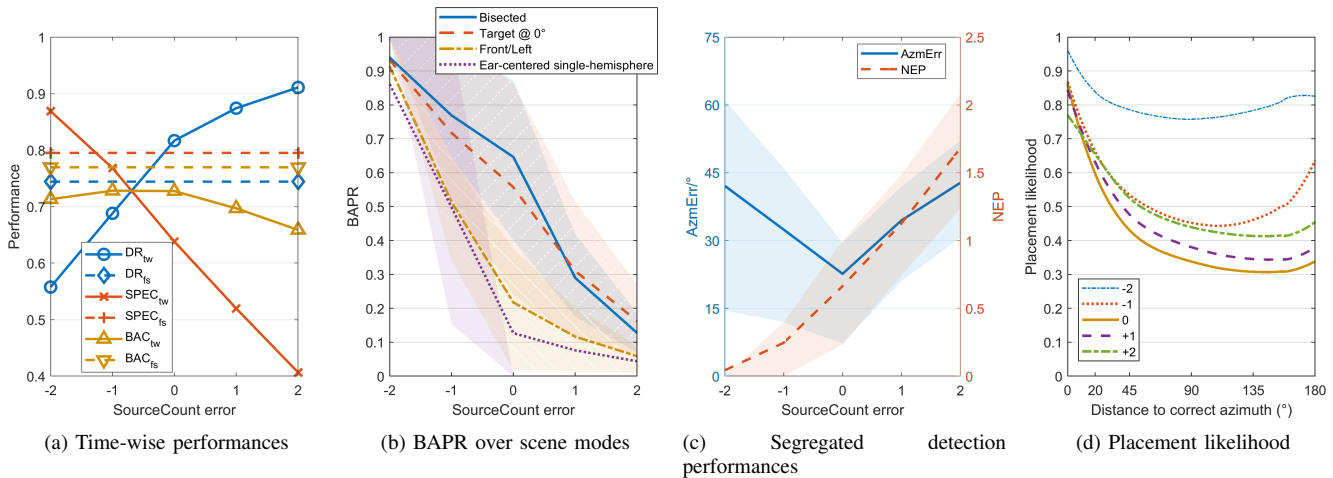


Fig. 7. Grand average (full test set, all test files, all classes) performances depending on strength of perturbation of source count information fed into the segregation model. Line plots display arithmetic means and, shaded, 25th to 75th percentiles. Table I or Section II-I provide descriptions of the presented measures.

The choice of training performance measure has a crucial impact on system performance in any machine learning model. Compared to employing standard BAC , that does not distinguish between N_{pp} and N_{npp} samples and hence would result in models largely unable to assign events to only the correct stream, the proposed BAC_{sw} has shown to produce functioning models. However, there may as well be more suitable measures; in particular, BAC_{sw} does not impose cost on azimuth distance of positive assignments¹². This would be an interesting point for further research.

Because of the significantly lower time-wise specificity, it may be beneficial to combine segregated detection models for localized detection together with fullstream detection models for actual sound event presence detection. The latter would prime or even trigger the application of segregated detection. [9] basically do the same to reduce false positives.

A diverse set of test scenes for thorough study of the behavior and conditions of good performance was defined along with several performance indicators to enable capturing different qualitative aspects of the joint behavior of the combined models. They can serve, together with the code, as testbed and benchmarks for alike systems with different components and other approaches to the problem, and of course particularly for spatial segregation and sound event detection models. All algorithms and tools for training, testing and evaluation, the sound data and the trained models themselves are provided as public domain ([30], [33], [56]).

ACKNOWLEDGMENT

This work was part of the TWO!EARS project funded by the European Union’s Seventh Framework Programme for research, technological development and demonstration under grant agreement no 618075.

¹²Other than discriminating between correct or incorrect stream

REFERENCES

- [1] K. Lopatka, J. Kotus, and A. Czyzewski, “Detection, classification and localization of acoustic events in the presence of background noise for acoustic surveillance of hazardous situations,” *Multimedia Tools and Applications*, vol. 75, no. 17, pp. 10407–10439, 2016.
- [2] T. Butko, F. G. Pla, C. Segura, C. Nadeu, and J. Hernando, “Two-source acoustic event detection and localization: Online implementation in a smart-room,” in *Signal Processing Conference, 2011 19th European*. IEEE, 2011, pp. 1317–1321.
- [3] N. Ma, J. A. Gonzalez, and G. J. Brown, “Robust Binaural Localization of a Target Sound Source by Combining Spectral Source Models and Deep Neural Networks,” *IEEE/ACM Transactions on Audio Speech and Language Processing*, vol. 26, no. 11, pp. 2122–2131, 2018.
- [4] R. Chakraborty and C. Nadeu, “Sound-model-based acoustic source localization using distributed microphone arrays,” in *2014 IEEE International Conference on Acoustics, Speech and Signal Processing (ICASSP)*. IEEE, 2014, pp. 619–623.
- [5] C. Grobler, C. Kruger, B. Silva, and G. Hancke, “Sound based localization and identification in industrial environments,” in *IECON 2017-43rd Annual Conference of the IEEE Industrial Electronics Society*. IEEE, 2017, pp. 6119–6124.
- [6] T. May, S. van de Par, and A. Kohlrausch, “A binaural scene analyzer for joint localization and recognition of speakers in the presence of interfering noise sources and reverberation,” *IEEE Transactions on Audio, Speech, and Language Processing*, vol. 20, no. 7, pp. 2016–2030, 2012.
- [7] T. Hirvonen, “Classification of spatial audio location and content using convolutional neural networks,” in *Audio Engineering Society Convention 138*, 2015.
- [8] W. He, P. Motlicek, and J.-M. Odobez, “Joint localization and classification of multiple sound sources using a multi-task neural network,” in *Proc. Interspeech 2018*, 2018, pp. 312–316.
- [9] S. Adavanne, A. Politis, J. Nikunen, and T. Virtanen, “Sound event localization and detection of overlapping sources using convolutional recurrent neural networks,” *IEEE Journal of Selected Topics in Signal Processing*, 2018.
- [10] H.-M. Park, C. S. Dhir, D.-K. Oh, and S.-Y. Lee, “Filterbank-based blind signal separation with estimated sound direction,” in *2005 IEEE International Symposium on Circuits and Systems*, 2005, pp. 5874–5877 Vol. 6.
- [11] H. Do and H. F. Silverman, “A robust sound-source separation algorithm for an adverse environment that combines mvdr-phat with the casa framework,” in *2011 IEEE Workshop on Applications of Signal Processing to Audio and Acoustics (WASPAA)*, 2011, pp. 273–276.
- [12] M. Maazaoui, Y. Grenier, and K. Abed-Meraim, “From binaural to multimicrophone blind source separation using fixed beamforming with hrfts,” in *2012 19th International Conference on Systems, Signals and Image Processing (IWSSIP)*, 2012, pp. 480–483.

- [13] I. Nakanishi and J. Hanada, "A sequential processing model for speech separation based on auditory scene analysis," in *2015 International Symposium on Intelligent Signal Processing and Communication Systems (ISPACS)*, 2015, pp. 124–128.
- [14] K. J. Faller, J. Riddley, and E. Grubbs, "Automatic blind source separation of speech sources in an auditory scene," in *2017 51st Asilomar Conference on Signals, Systems, and Computers*, 2017, pp. 248–250.
- [15] D. Kolossa and R. Orgmeister, "Nonlinear postprocessing for blind speech separation," in *International Conference on Independent Component Analysis and Signal Separation*. Springer, 2004, pp. 832–839.
- [16] N. Harishkumar and R. Rajavel, "Monaural speech separation system based on optimum soft mask," in *2014 IEEE International Conference on Computational Intelligence and Computing Research*, 2014, pp. 1–4.
- [17] I. Trowitzsch, J. Mohr, Y. Kashef, and K. Obermayer, "Robust detection of environmental sounds in binaural auditory scenes," *IEEE/ACM Transactions on Audio, Speech, and Language Processing*, vol. 25, no. 6, pp. 1344–1356, 2017.
- [18] L. Hertel, H. Phan, and A. Mertins, "Comparing time and frequency domain for audio event recognition using deep learning," in *Neural Networks (IJCNN), 2016 International Joint Conference on*. IEEE, 2016, pp. 3407–3411.
- [19] H. Phan, L. Hertel, M. Maass, and A. Mertins, "Robust audio event recognition with 1-max pooling convolutional neural networks," in *Proceedings of the Annual Conference of the International Speech Communication Association, INTERSPEECH*, no. 1, 2016, pp. 3653–3657.
- [20] E. Cakir and T. Virtanen, "Convolutional Recurrent Neural Networks for Rare Sound Event Detection," in *DCASE 2017 Proceedings*, no. 11, 2017, pp. 1–5.
- [21] I.-Y. Jeong, S. Lee, Y. Han, and K. Lee, "Audio event detection using multiple-input convolutional neural network," *Detection and Classification of Acoustic Scenes and Events (DCASE)*, 2017.
- [22] T. Hayashi, S. Watanabe, T. Toda, T. Hori, J. Le Roux, and K. Takeda, "Duration-controlled lstm for polyphonic sound event detection," *IEEE/ACM Transactions on Audio, Speech and Language Processing (TASLP)*, vol. 25, no. 11, pp. 2059–2070, 2017.
- [23] B. Li, T. N. Sainath, A. Narayanan, J. Caroselli, M. Bacchiani, A. Misra, I. Shafraan, H. Sak, G. Pundak, K. Chin, K. C. Sim, R. J. Weiss, K. W. Wilson, E. Variiani, C. Kim, O. Siohan, M. Weintraub, E. McDermott, R. Rose, and M. Shannon, "Acoustic modeling for Google home," in *Proceedings of the Annual Conference of the International Speech Communication Association, INTERSPEECH*, 2017, pp. 399–403.
- [24] T. Virtanen, A. Mesaros, T. Heittola, M. Plumbley, P. Foster, E. Benetos, and M. Lagrange, Eds., *Proceedings of the Detection and Classification of Acoustic Scenes and Events 2016 Workshop (DCASE2016)*. Tampere University of Technology, Department of Signal Processing, 2016.
- [25] T. Virtanen, A. Mesaros, T. Heittola, A. Diment, E. Vincent, E. Benetos, and B. M. Elizalde, Eds., *Proceedings of the Detection and Classification of Acoustic Scenes and Events 2017 Workshop (DCASE2017)*. Tampere University of Technology, Laboratory of Signal Processing, 2017.
- [26] M. D. Plumbley, C. Kroos, J. P. Bello, G. Richard, D. P. Ellis, and A. Mesaros, Eds., *Proceedings of the Detection and Classification of Acoustic Scenes and Events 2018 Workshop (DCASE2018)*. Tampere University of Technology, Laboratory of Signal Processing, 2018.
- [27] A. Raake, J. Blauert, J. Braasch, G. Brown, P. Dans, T. Dau, B. Gas, S. Argentieri, A. Kohlrausch, D. Kolossa, N. Le Goff, T. May, K. Obermayer, C. Schymura, T. Walther, H. Wierstorf, F. Winter, and S. Spors, "Two'ears – integral interactive model of auditory perception and experience," 2014.
- [28] O. Nadiri and B. Rafaely, "Localization of multiple speakers under high reverberation using a spherical microphone array and the direct-path dominance test," *IEEE/ACM Transactions on Audio, Speech, and Language Processing*, vol. 22, no. 10, pp. 1494–1505, 2014.
- [29] S. Gannot, E. Vincent, S. Markovich-Golan, and A. Ozerov, "A consolidated perspective on multimicrophone speech enhancement and source separation," *IEEE/ACM Transactions on Audio, Speech, and Language Processing*, vol. 25, no. 4, pp. 692–730, 2017.
- [30] I. Trowitzsch, J. Taghia, Y. Kashef, and K. Obermayer, "The NIGENS General Sound Events Database," Technische Universitt Berlin, Tech. Rep., 2019. [Online]. Available: <https://arxiv.org/abs/1902.08314>
- [31] T. Team. (2018) Two'ears auditory model 1.5. [Online]. Available: <https://doi.org/10.5281/zenodo.1458420>
- [32] H. Wierstorf, M. Geier, and S. Spors, "A free database of head related impulse response measurements in the horizontal plane with multiple distances," in *Audio Engineering Society Convention 130*, 2011.
- [33] I. Trowitzsch, Y. Kashef, and K. Obermayer. (2019) Auditory Machine Learning Training and Testing Pipeline: AMLTTP v3.0. [Online]. Available: <https://doi.org/10.5281/zenodo.2575086>
- [34] A. J. Dobson, *An introduction to generalized linear models*, 2nd ed. Chapman & Hall/CRC Boca Raton, 2002.
- [35] J. K. Nielsen, M. G. Christensen, and S. H. Jensen, "Bayesian model comparison and the bic for regression models," in *2013 IEEE International Conference on Acoustics, Speech and Signal Processing*, 2013, pp. 6362–6366.
- [36] B. R. Glasberg and B. C. Moore, "Derivation of auditory filter shapes from notched-noise data," *Hearing research*, vol. 47, no. 1-2, pp. 103–138, 1990.
- [37] R. D. Patterson and J. Holdsworth, "A functional model of neural activity patterns and auditory images," *Advances in speech, hearing and language processing*, vol. 3, no. Part B, pp. 547–563, 1996.
- [38] M. Cooke, P. Green, L. Josifovski, and A. Vizinho, "Robust automatic speech recognition with missing and unreliable acoustic data," *Speech communication*, vol. 34, no. 3, pp. 267–285, 2001.
- [39] G. Peeters, B. L. Giordano, P. Susini, N. Misdariis, and S. McAdams, "The timbre toolbox: Extracting audio descriptors from musical signals," *The Journal of the Acoustical Society of America*, vol. 130, no. 5, pp. 2902–2916, 2011.
- [40] G. Tzanetakis and P. Cook, "Musical genre classification of audio signals," *IEEE Transactions on speech and audio processing*, vol. 10, no. 5, pp. 293–302, 2002.
- [41] K. Jensen and T. H. Andersen, "Real-time beat estimation using feature extraction," in *International Symposium on Computer Music Modeling and Retrieval*. Springer, 2003, pp. 13–22.
- [42] H. Misra, S. Iqbal, H. Bourlard, and H. Hermansky, "Spectral entropy based feature for robust asr," in *Proceedings of IEEE International Conference on Acoustics, Speech, and Signal Processing (ICASSP)*, 2004.
- [43] A. Lerch, *An introduction to audio content analysis: Applications in signal processing and music informatics*. John Wiley & Sons, 2012.
- [44] J. T. Geiger, B. Schuller, and G. Rigoll, "Large-scale audio feature extraction and svm for acoustic scene classification," in *2013 IEEE Workshop on Applications of Signal Processing to Audio and Acoustics*, 2013, pp. 1–4.
- [45] E. Marchi, D. Tonelli, X. Xu, F. Ringeval, J. Deng, and B. Schuller, "The up system for the 2016 DCASE challenge using deep recurrent neural network and multiscale kernel subspace learning," DCASE2016 Challenge, Tech. Rep., 2016.
- [46] N. Moritz, J. Anemller, and B. Kollmeier, "Amplitude modulation spectrogram based features for robust speech recognition in noisy and reverberant environments," in *2011 IEEE International Conference on Acoustics, Speech and Signal Processing (ICASSP)*. IEEE, 2011, pp. 5492–5495.
- [47] T. May and T. Dau, "Computational speech segregation based on an auditory-inspired modulation analysis," *The Journal of the Acoustical Society of America*, vol. 136, no. 6, pp. 3350–3359, 2014.
- [48] J. R. Hosking, "L-moments: analysis and estimation of distributions using linear combinations of order statistics," *Journal of the Royal Statistical Society. Series B (Methodological)*, pp. 105–124, 1990.
- [49] H. A. David and H. N. Nagaraja, *Order Statistics*, 3rd ed. Wiley, 2003.
- [50] R. Tibshirani, "Regression shrinkage and selection via the lasso," *Journal of the Royal Statistical Society. Series B (Methodological)*, pp. 267–288, 1996.
- [51] J. Friedman, T. Hastie, and R. Tibshirani, "Regularization paths for generalized linear models via coordinate descent," *Journal of statistical software*, vol. 33, no. 1, p. 1, 2010.
- [52] J. Qian, T. Hastie, J. Friedman, R. Tibshirani, and N. Simon. (2013) Glmnet for matlab. [Online]. Available: <http://gts.sourceforge.net/>
- [53] D. M. H. Powers, "Evaluation: From Precision, Recall and F-Measure To Roc, Informedness, Markedness & Correlation," *Journal of Machine Learning Technologies*, vol. 2, no. 1, pp. 37–63, 2011.
- [54] W. J. Youden, "Index for rating diagnostic tests," *Cancer*, vol. 3, no. 1, pp. 32–35, 1950.
- [55] N. Ma, T. May, and G. J. Brown, "Exploiting Deep Neural Networks and Head Movements for Robust Binaural Localization of Multiple Sources in Reverberant Environments," *IEEE/ACM Transactions on Audio Speech and Language Processing*, vol. 25, no. 12, pp. 2444–2453, 2017.
- [56] I. Trowitzsch. (2019) Supplementary materials to TASLP: SELD through spatial segregation. [Online]. Available: <https://github.com/nigroup/Supplementaries-to-TASLP-SELD-Spatial-Segregation>

Ivo Trowitzsch received his Diplom degree in Computer Engineering from the Technische Universität Berlin, Germany, in 2011. He is a graduate research assistant at the Neural Information Processing Group at Technische Universität Berlin. His research interests currently focus on the application of machine learning in computational auditory scene analysis and in general audio processing.

Christopher Schymura (S'13—M'17) received the Dipl.-Ing. degree in electrical engineering and information technology from Ruhr University Bochum, Germany, in 2013. Since 2013, he has been working as a research assistant at the Cognitive Signal Processing group, Institute of Communication Acoustics at Ruhr University Bochum. His research interests include machine learning and probabilistic modeling for multimodal signal processing and robotics.

Dorothea Kolossa Dorothea Kolossa received the Dipl.-Ing. degree in computer engineering and the Dr.-Ing. degree in electrical engineering from Technische Universität Berlin, Germany, in 1999 and 2007, respectively. From 1999 until 2000, she worked on control systems design at DaimlerChrysler Research and Technology, Hennigsdorf, Germany. She was employed as a research assistant at Technische Universität Berlin from 2000 until 2004, and as a senior researcher from 2004 until 2010, also staying at UC Berkeley's Parlab as visiting faculty in 2009/2010. Since 2010, she has been working in a faculty position at the Institute of Communication Acoustics, Ruhr-Universität Bochum, Germany, where currently, she is heading the Cognitive Signal Processing group as an associate professor. Her research interests include speech recognition in adverse environments and robust classification methods for communication and technical diagnostics. She has authored and co-authored more than 100 scientific papers and book chapters. Dr. Kolossa is a member of the Council of the EAA TC on Audio Signal Processing, and of the IEEE Audio and Acoustic Signal Processing Technical Committee.

Klaus Obermayer Klaus Obermayer received his Diplom degree in physics in 1987 from the University of Stuttgart, Germany, and the Dr. rer. nat. degree in 1992 from the Department of Physics, Technical University of Munich, Germany. From 1992 and 1993 he was a postdoctoral fellow at the Rockefeller University, New York, and the Salk Institute for Biological Studies, La Jolla, USA. From 1994 to 1995 he was member of the Technische Fakultät, University of Bielefeld, Germany. He became associate professor in 1995 and full professor in 2001 at the Department of Electrical Engineering and Computer Science of the Berlin University of Technology, Germany. He is head of the Neural Information Processing Group and member of the steering committee of the Bernstein Center for Computational Neuroscience Berlin. He was member of the governing board of the International Neural Network Society from 2004 - 2012 and was Vice-President of the Organisation for Computational Neuroscience from 2008-2011. From 1999-2003 he was one of the directors of the European Advanced Course of Computational Neuroscience. His current areas of research are computational neuroscience, artificial neural networks and machine learning, and the analysis of neural data. He co-authored more than 250 scientific publications.